AN ANALYSIS OF PRESSURE DROPS IN WELLBORE, UNDER LOW FLOW RATE CONDITIONS, SHOWN ON A DELIVERABILITY CURVE

KHASANI', R. ITOI', T. TANAKA[1], & M. FUKUDA[2]

[1]Dept. of Earth Resources Engineering, Graduate School of Engineering, Kyushu University, Fukuoka, Japan
[2]Laboratory of Energy Resources Engineering, Graduate School of Engineering, Kyushu University, Fukuoka, Japan

SUMMARY – This study investigated pressure drops in wellbore under low flow rate conditions and shows them on a deliverability curve. A simple model of a vertical wellbore of uniform diameter, coupled with a reservoir of uniform, radial, horizontal thickness was employed. The momentum equation for two-phase flow in a wellbore was numerically evaluated using a method introduced by Orkiszewski (1967). Isenthalpic conditions were assumed for the energy equation. The numerical calculation showed that at low flow rates, the pressure drops in the wellbore were dominated by a potential pressure drop component then followed by a fkiction component and finally an acceleration component. As the flow rate increased the potential pressure drop decreased while the two other components tended to increase. The decrease in the total flow rate results in a decrease in the slug regime length in the wellbore.

1. INTRODUCTION

When developing geothermal energy for power generation, it is important for the reservoir engineers to understand the well performance and to evaluate the well deliverability. Predicting the steam discharge rate from wells, and evaluating the effects of reservoir conditions on the steam flow rate provides valuable information when defining the size of power plant. A deliverability curve is one of the tools used for the evaluation of well performance. It expresses the relationship between wellhead pressure and mass flow rate. The possible variations of the deliverability curve depend on many factors, such as: the type of reservoir, the permeability, the reservoir pressure and temperature, the gas content, and amount of scaling in the wellbore.

A typical deliverability curve is characterized by the existence of a maximum discharge pressure. The experience in Wairakei showed that the wellhead pressures could only be raised to a certain maximum value by throttling discharge. Raising it beyond this results in the collapse of the flowing steam-water mixture and closure of the well corresponding to the maximum value of discharge pressure (James, 1980). Another type of deliverability curve at Well 10 in the Svartsengi field showed the decrease in wellhead pressure as well as mass flow rate for low flow rate conditions (Gudmundsson *et al.,* 1981).

Grant *et al.* (1982) qualitatively discussed the collapse of the discharge by throttling from a large flow. However, a quantitative analysis provides a better understanding. This paper deals with the mechanisms through a numerical study; it investigates why the deliverability curve changes to decreasing WHP as the flow rate declines after reaching the maximum discharge pressure.

2. GOVERNING EQUATIONS

The schematic of the reservoir and wellbore model is illustrated in Figure 1. The governing equations consist of those for the wellbore that are coupled with the fluid flow in a reservoir.

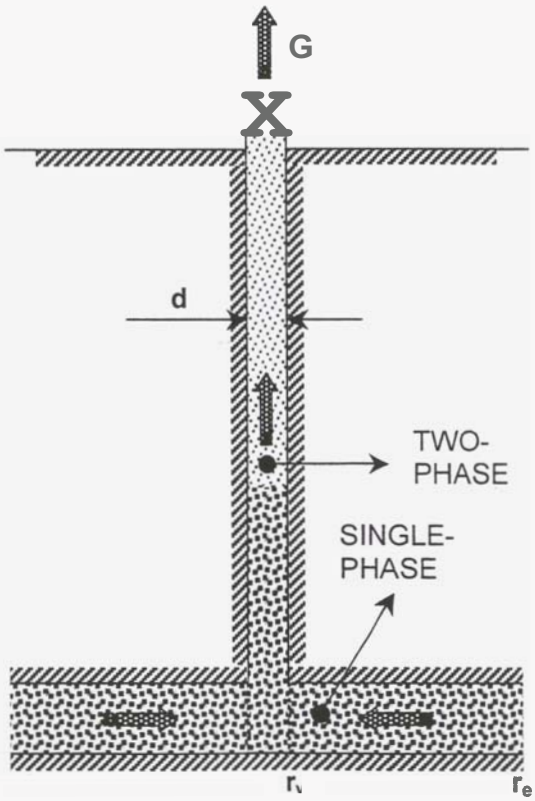

Figure 1 - Schematic of the Reservoir-Wellbore Model.

2.1 Equations for the Reservoir

Basic equations for fluid flow in the reservoir are derived using the following assumptions (Itoi *et al.*, 1988):

(1) the reservoir is of radial symmetry and has a constant horizontal thickness
(2) the fluid flow obeys Darcy's law and is under steady state
(3) there is no heat exchange between the fluid and reservoir rock, and the flow is isenthalpic.

Continuity equations of mass and momentum in the reservoir are expressed as:

$$-\frac{1}{r}\frac{\partial(ru)}{\partial r}=0 \qquad (1)$$

For single-phase: $u=-\frac{k}{\nu_w}\frac{\partial p}{\partial r}$ (2)

For two-phase: $u=-\frac{k}{\nu_t}\frac{\partial p}{\partial r}$ (3)

where r : radial distance (m), u : mass flux density (kg/m^{2}s), p : pressure (Pa), k : permeability (m^2), ν_w : kinematic viscosity of water (m^2/s), ν_t : total kinematic viscosity of two-phase fluid (m^2/s).

Mass flux density is the sum of steam and water flux densities (u_s and u_w) written as:

$$u=u_w+u_s=-\left(\frac{kk_{rw}}{\nu_w}+\frac{kk_{rs}}{\nu_s}\right)\frac{\partial p}{\partial r} \qquad (4)$$

where ν_s : kinematic viscosity of steam (m^2/s).
Then, the total kinematic viscosity can be defined (Grant et al., 1982):

$$\frac{1}{\nu_t}=\frac{k_{rw}}{\nu_w}+\frac{k_{rs}}{\nu_s} \qquad (5)$$

where k_{rw} : relative permeability to water (-), k_{rs} : relative permeability to steam (-).

By use of a definition of flowing enthalpy, relative permeabilities can be expressed using enthalpies of steam and water:

$$\frac{k_{rs}}{k_{rw}}=\frac{\nu_s(i_w-i)}{\nu_w(i-i_s)} \qquad (6)$$

where i : total enthalpy of fluid (J/kg), i_w : enthalpy of water (J/kg), i_s : enthalpy of steam (J/kg).

Relative permeabilities can be expressed as a function of water saturation in porous media or fractured media. In this study, the correlation between relative permeabilities is expressed in an X-curve that satisfies the following expression:

$$k_{rs}+k_{rw}=1 \qquad (7)$$

then, ν_t can be expressed:

$$\frac{1}{\nu_t}=\frac{(i_w-i_s)}{\nu_w(i-i_s)+\nu_s(i_w-i)} \qquad (8)$$

When fluid starts to flash in the reservoir, a liquid flow region and a two-phase flow region exist. The flow rate of the two-phase mixture entering the wellbore at the feed zone can be calculated:

$$G=-uA|_{r_w}=2\pi h\left(\frac{k}{\nu_t}\frac{\partial p}{\partial r}\right)_{r_w} \qquad (9)$$

where A : the surface area of the well at feed zone (m^2), h : reservoir thickness (m).

The boundary conditions are expressed as:

$$r=r_w \rightarrow p=p_{wb}$$
$$r=r_s \rightarrow p=p_{sat}$$
$$r=r_e \rightarrow p=p_e$$

where r_w : well radius (m), r_s : radius at which fluid starts flashing (m), r_e : outer boundary radius (m), p_{wb} : pressure at well bottom (Pa), p_{sat} : saturation pressure (Pa), p_e : pressure at outer boundary (Pa).

Because the total kinematic viscosity is a function of pressure, we need to evaluate the pressure gradients in Equation (9) for given mass flow rate to find a feed zone pressure, p_{wb}. Equation (9) can be rewritten with the boundary conditions above as follows.

$$G=2\pi kh\frac{\int_{p_{wb}}^{p_{sat}}\frac{\partial p}{\nu_t}}{R_s} \qquad (10)$$

where R_s is the normalized distance of r_s ($R_s=ln(r_s/r_w)$).

R_s is given by:

$$R_s=R_e-\frac{2\pi kh}{G\nu_w}(p_e-p_{sat}) \qquad (11)$$

where $R_e=ln(r_e/r_w)$.

When liquid flows into the well, its flow rate is expressed as:

$$G=-uA|_{R_w}=\frac{2\pi kh(p_e-p_{wb})}{\nu_w R_e} \qquad (12)$$

where $R_w=ln(r_w/r_w)$.

2.2 Equations for the Wellbore

Basic equations for fluid flow in the wellbore are derived using the following assumptions:

(1) the fluid flows into the well from a single feed zone at the well bottom
(2) the well is vertical with a uniform diameter
(3) the fluid flow in the well is under steady state and is isenthalpic.

The basic equations used for two-phase flow in the wellbore consist of mass and momentum equations as follows:

$$\frac{dM}{dl} = 0 \qquad (13)$$

$$\Delta P_t - \{\Delta P_a + \Delta P_h + \Delta P_f\} = 0 \qquad (14)$$

where M : total mass flow (kg/s), l : depth coordinate (m), ΔP_t : total pressure drop (Pa), ΔP_a : pressure drop due to acceleration (Pa), ΔP_h : pressure drop due to potential (Pa), ΔP_f : pressure drop due to fi-iction (Pa).

Each component of the pressure drop is evaluated as follows:

- Pressure drop due to potential (ΔP_h)

Potential loss for vertical two-phase flow in a small length increment ΔL (m) is given as:

$$\Delta P_h = \rho_m . g . \Delta L \qquad (15)$$

where ρ_m is the mixture density and evaluated using method introduced by Orkiszewski (1967) as well as velocity.

- Pressure drop due to acceleration (ΔP_a)

Acceleration loss for the two-phase flow with the specific volume of v_m between two points 1 and 2 with pressure different ΔP, is:

$$\Delta P_a = \left(\frac{M}{A}\right)^2 \left(v_{m,1} - v_{m,2}\right) \qquad (16)$$

- Pressure drop due to friction (ΔP_f)

Friction loss is calculated using the following equation:

$$\Delta P_f = \frac{\lambda_m}{2D} \frac{M^2}{\rho_m A^2} \Delta L \qquad (17)$$

where λ_m is the friction factor for two-phase flow and evaluated using equations proposed by Swamee & Jain (Lindeburg, 1992):

$$a_s = \frac{64}{Re} \quad \text{for } Re < 2100 \qquad (18)$$

$$\lambda_m = \frac{0.25}{\left[log_{10}\left(\frac{\varepsilon / D}{3.7} + \frac{5.74}{Re^{0.9}}\right)\right]^2} \quad \text{for } Re > 2100 \qquad (19)$$

where Re is the Reynolds number that depends on well diameter, fluid velocity, fluid density and dynamic viscosity of fluid and ε is the pipe roughness. In order to evaluate the above fluid parameters, the void ratio must be first determined.

3. CALCULATION PROCEDURE

3.1 Input Parameters for Calculation

The parameters for the reservoir and wellbore used in this study are shown in Table 1.

Table 1 Reservoir and Wellbore Parameters

Reservoir	Wellbore
Pressure 80 bar	Diameter 0.2 m
Temperature 280°C	Length 1000 m
Horizontal Extent 50 m	Roughness 0.000046 m
Permeability Thickness 1 – 5 darcy-m	

3.2 Calculation Procedure

Firstly, read the input data from both the reservoir and wellbore. Secondly, check the reservoir to determine whether it is in a single-phase or two-phase condition, by comparing the reservoir pressure and saturation pressure for the given reservoir temperature. The main objective of this reservoir calculation is to obtain a mass flow rate and a well bottom pressure, which are then used as input data for the wellbore calculation.

Basically, the wellbore calculation computes the total pressure drop in the wellbore that depends on the flow regimes. The wellbore is divided into small segments of pressure increment ΔP, then the corresponding length increment ΔL is calculated. All fluid thermodynamic properties in each segment are evaluated in the average values. The main objective of this calculation is to get the wellhead pressure. Other results can also be obtained, such as the wellhead enthalpy, dryness, etc.

4. RESULTS AND DISCUSSION

4.1 Deliverability Curves for Different kh

Deliverability curves for different permeability thicknesses (kh) are obtained from the reservoir and wellbore calculation for mass flow rate and wellhead pressure (WHP), and are shown in Figure 2.

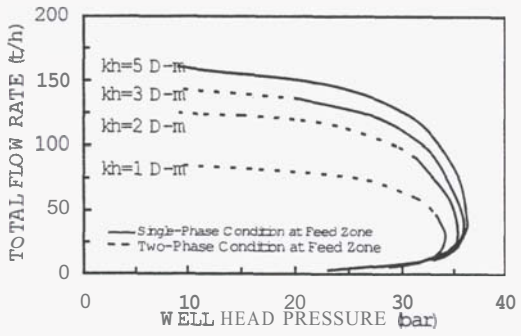

Figure 2 - WHP vs Total Flow Rate

From Figure 2, it can be seen that for the low flow rate an increase in the wellhead pressure is followed by an increase in the total flow rate until it reaches the maximum pressure. Any further increase in the total flow rate results in a decrease in the wellhead pressure. The solid line represents single-phase fluid entering the wellbore while the dashed line indicates a two-phase flow entering the wellbore. The two-phase flow rate at the feed zone increases as the permeability thickness increases The presence of the maximum wellhead pressure, as shown in the figure; creates conditions at which there is a certain wellhead pressure value that gives two different total flow rate values. To explain this phenomenon, especially for low flow rate conditions, we performed a quantitative analysis of the pressure calculation in the wellbore, discussed in the next section.

4.2 Analysis of Pressure Drops

To explain the mechanism as to how the deliverability curve turns at maximum discharge pressure, we can analyze the pressure drops in wellbore which are shown in Table 2.

From Table 2 it can be seen that under low flow rate conditions, most of pressure drop in the wellbore is dominated by potential pressure loss, then followed by friction, and finally by acceleration. It can also be seen that as the flow rate increases, the potential loss decreases; while on the other hand, acceleration and friction losses increase. These pressure loss relationships may cause the presence of the two different kinds of flow rate at the same WHP.

4.3 Pressure Distributions in Wellbore

To qualitatively analyze the phenomenon occurring at low flow rates, we examined the pressure profile under those conditions. Figure 3 shows the pressure profiles in the wellbore for the different flow rate conditions. The reservoir conditions used in the calculation are: reservoir pressure of 80 bar, reservoir temperature of 280°C, and permeability thickness (kh) of 3 D-m. The wellbore diameter is 0.2 m and the wellbore length is 1000 m.

From Figures 3 (a), (b), and (c), it was found that each wellhead pressure gives two different feed zone pressures and flow rates. All curves show slug flow regime at wellhead, no matter what flow regime enters the wellbore. The only differences are the depth of flashing. As the flow rate increases, the flashing point moves deeper. It was also observed that the lengths of slug and bubble regimes decrease. This phenomenon indicates that for the lower flow rate, the flashing point occurs closer to the wellhead. Using this specific flow rate condition, we can explain the possible collapse of discharge. as discussed by Grant et *al.* (1982). At this low flow rate condition, steam bubbles rise through water and provide buoyancy or steam-lift to raise the water to the wellhead. If the flow decreases, it may approach a speed at which the water velocity up the well is too slow for the steam bubbles rising through water to provide much steam-lift. Any further decrease in the flow rate results in insufficient steam-lift to maintain the upflow of water, and the discharge will stop.

To analyze the phenomena where there should be a minimum flow rate so that the well can sustain the discharge, the concept of onset of flow rate (flooding) will improve understanding. Park *et al.* (1998) discussed a physical model that provides a comprehensive understanding of the critical heat flow characteristics to help predict their values under zero and very low flow conditions.

For future work, concepts such as those discussed above may be applied on an actual geothermal wellbore.

Table **2** Pressure Losses Component for kh=3 darcy-m.

Total Flow Rate (t/h)	Wellhead Pressure (bar)	Pressure Loss Component (%)		
		$\Delta P_h/\Delta P_t$	$\Delta P_a/\Delta P_t$	$\Delta P_f/\Delta P_t$
4	25	99.97	0.01	0.02
7	30	99.9	0.03	0.07
21	35	97.8	1.67	0.53
67	35	92.8	1.93	5.27
112	30	74.5	7.2	18.3
128	25	59.9	11.9	28.2

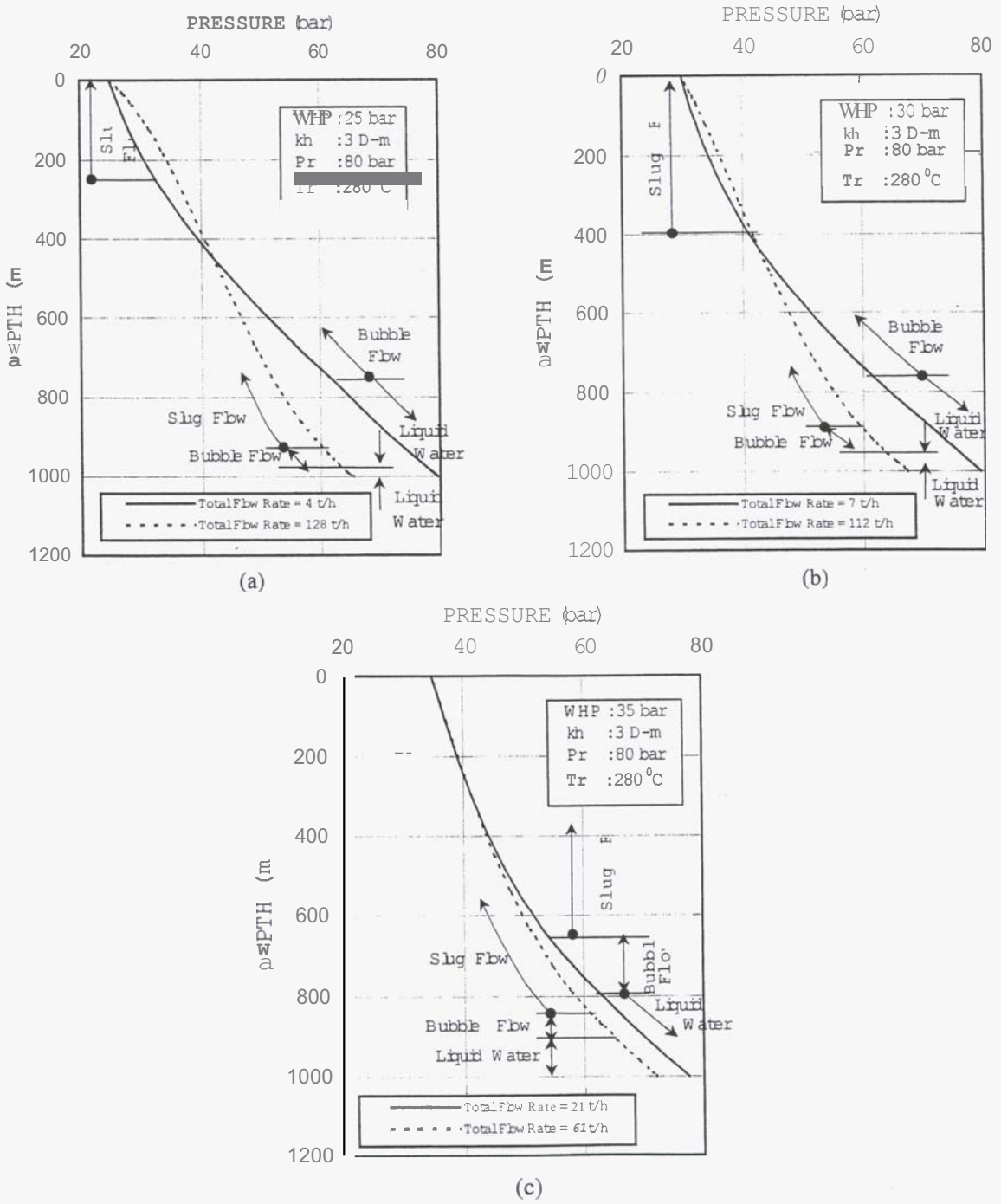

Figure **3** - Pressure Distribution in Wellbore: (a) WHP: **25** bar, (b) WHP: **30** bar, (c) WHP: **35** bar

5. CONCLUSIONS

From the analyses of the results, the following conclusions have been drawn:

(1) The numerical calculations show that at low flow rates the pressure drops in the wellbore are dominated by a potential pressure drop component, then followed by a friction component, and finally by an acceleration component.

(2) As the flow rate increased the potential drop decreased, while the other two component values tended to increase.

(3) The decrease in the total flow rate produces the decrease in the slug regime length.

(4) There should be a minimum flow rate (onset of flow rate) so that the well can sustain discharge.

6. ACKNOWLEDGEMENTS

The first author gratefully acknowledges the financial support of the Ministry of Education, Culture, Sports, Science and Technology, Government of Japan in the form of a scholarship, enabling the first author to attend the masters and doctorate courses at the Dept. of Earth Resources Engineering, Graduate School of Engineering, Kyushu University.

7. REFERENCES

Grant M.A., Donaldson, I.G., and Bixley, P.F. (1982) *Geothermal Reservoir Engineering.* Academic Press, 369p.

Gudmunsson, J.S., Thorhallsson, S., and Ragnars, K. (1981) Status of Geothermal Electric Power in Iceland 1980. *Proc. 5th Geoth. Conf. Workshop, Electric Power Research Institute,* Report AP-2098, Nov. 1981.

Itoi, R., Kakihara, Y., Fukuda, M., and Koga, A. (1988) Numerical Simulation of Well Characteristics Coupled with Radial Flow in a Geothermal Reservoir. *International Symposium on Geothermal Energy,* Kumamoto and Beppu, Japan, pp.201-204.

James, R. (1980) Significance of the. Maximum Discharging-Pressure of Geothermal Wells. *Proc. 6th Workshop Geothermal Reservoir Engineering, Stanford Geothermal Program,* pp. 145-149.

Lindeburg, M.R. (1992) *Engineering – Training Reference Manual.* 8th Edition. Professional Publications, Inc., 933p.

Orkiszewski, J. (1967) Predicting Two-Phase Pressure Drops in Vertical Pipe. *Journal of Petroleum Technology,* pp. 829-838.

Park, C., Hyun Hwan D. (1998) An Improved Physical Model for Flooding Limited CHF under Zero and Very Low Flow Conditions. *Int. Comm. Heat Mass Transfer,* Vol. 25, No.3, pp. 339-348.